JOURNAL OF CATALYSIS **180,** 225–233 (1998)
ARTICLE NO. CA982258

Plasma Decomposition of CO_2 in the Presence of Metal Catalysts

Stephanie L. Brock,* Manuel Marquez,*,‡ Steven L. Suib,*,†,[1] Yuji Hayashi,§ and Hiroshige Matsumoto¶

*Department of Chemistry, U-60, †Department of Chemical Engineering and Institute of Materials Science, University of Connecticut, Storrs, Connecticut 06269-4060; ‡Department of Electrical Engineering and Applied Physics, Yale University, New Haven, Connecticut 06511; ¶Department of Chemistry, Nagasaki University, Bunkyomachi 1-14, Nagasaki, 852, Japan; and §Fujitsu Laboratories Limited, 1015 Kamikodanaka, Nakahara, 211, Japan

Received May 4, 1998; revised August 10, 1998; accepted August 13, 1998

The decomposition of CO_2 in fan-type ac glow discharge plasma reactors coated with gold, copper, platinum, palladium, rhodium, and mixed rotor/stator systems (Au/Rh and Rh/Au) was investigated. A high-voltage ac signal was used to produce a plasma between the fins of a turning rotor and an immobile stator, through which a 2.5% CO_2 in He mixture was passed. The analysis of the product gases was achieved using a mass spectrometer equipped with a partial pressure analyzer, and the decomposition of CO_2 was found to proceed to CO and O_2 with >80% selectivity. The percentage conversion of CO_2 increases with decreasing flow rate and increasing input voltage. The opposite trend is obtained when the energy efficiency is evaluated. Spectroscopic data indicate that the diluent gas plays a role in the dissociation of CO_2, likely via charge and energy transfer from excited state He species to produce vibrationally excited CO_2^+ intermediates. The order of reactivity for the different metal catalyst coatings is Rh > Pt ≈ Cu > Pd > Au/Rh ≈ Rh/Au ≈ Au. With the Rh-coated reactor, conversions as high as 30.5%, reaction rates of 8.07×10^{-4} mol/h, and energy efficiencies of 3.55% could be obtained. There is a clear relationship between excitation temperature, T_{ex}, of a pure He plasma and the conversion of CO_2 in a CO_2/He plasma: decreasing T_{ex} corresponds to increasing conversion.

INTRODUCTION

Carbon dioxide is a main contributor to the greenhouse effect and man-made sources produce 30 gigatons per year, largely from combustion of fossil fuels (1). Control of emission from automobiles and power plants is a global concern (2–4), and as such, feasible technologies for large-scale remediation of carbon dioxide have recently become an active area of research. As CO_2 is the end product of complete combustion of organic compounds, its utilization in chemical production or energy production (as in methane reforming) may involve reduction of CO_2 to CO (5). A number of groups have looked at CO_2 for methane reforming (6–8); however, as CO_2 is very inert, the reaction requires a large energy input. Hydrogenation of CO_2 to produce petrochemical feed stocks has also been extensively explored (5, 9), but the high cost of hydrogen has limited most applications. Additionally, since hydrogen is commonly produced from the water–gas-shift reaction, which produces CO_2 as a by-product, this is not a viable method of reducing CO_2 from the atmosphere (1). Thus, to decrease emission of CO_2 into the environment, a method for reduction which does not require fossil fuel sources is needed.

Plasmas easily break down CO_2 into CO or coke. Initially, research was conducted on low-pressure plasmas containing CO_2. The processes for CO and coke formation have been well studied in these systems (10, 11), as well as the effect of additional gaseous components, such as hydrogen, argon, and nitrogen on the dissociation of CO_2 (12). Plasma processes are ideal for decomposition of CO_2.

Within a plasma, the vibrational, electronic, and rotational temperatures can all be different. With sufficient control, energy can be used to selectively produce vibrationally excited CO_2. The presence of vibrationally excited CO_2 in the plasma results in dissociation via electron impact with as little as 0.1 eV (13, 14). In contrast, ground state CO_2 requires >5.2 eV for dissociation via electron impact (15). Thus, plasma remediation of CO_2 can be energy efficient relative to other methods. However, for practical applications of plasmas for decomposition of CO_2 from flue gases, a plasma reactor operating at atmospheric pressure is desirable. Chang and co-workers have explored the use of corona-torch (16) and packed bed plasma reactors (14) for atmospheric pressure reduction of CO_2 and have been able to remove up to 0.108 kg of CO_2 per kilowatt hour of applied power from gas mixtures that mimic flue emissions (14).

We have long studied the use of low-pressure microwave plasmas for oligomerization of light hydrocarbons (17, 18). Recently, we have turned our attention to the use of atmospheric pressure plasmas for the remediation of pollutant gases and the synthesis of new materials (19) using fan-type ac glow discharge plasma reactors (20, 21). A plasma is generated by application of ac high voltage across a gap

[1] To whom correspondence should be addressed.

0021-9517/98 $25.00

(0.3 mm) between the rotor and the stator of a fan. The presence of the fan operating at high revolutions per minute (rpm) makes the reactor suitable for use under sluggish flow conditions. Additionally, the fans can be coated with a variety of metals or metal oxides which may act as catalysts. A variety of researchers have observed significant improvement in conversion and selectivity when plasmas are operated in the presence of metal and metal oxide catalysts, suggesting that synergistic effects may be at work (22, 23).

Here we report the decomposition of CO_2 using fan-type plasma reactors coated with rhodium, platinum, palladium, copper, and gold for a 2.5% CO_2 in He gas mixture. The effects of input voltage, flow rate, and metal coating on the conversion, reaction rate, and energy efficiency of CO_2 decomposition will be discussed. Spectroscopic studies of the plasmas will also be presented and probable mechanisms for CO_2 decomposition considered.

EXPERIMENTAL

Plasma reactor. CO_2 decomposition reactions were run in *p*lasma *a*nd *c*atalysis *i*ntegrated *t*echnologies (PACT) fan-type reactors. The reactor consists of an inner rotor with a diameter of 5.59 cm, a width of 1.66 cm, and 10 evenly spaced fan blades which protrude 0.34 cm from the fan. The stator has an inner diameter of 6.33 cm producing a gap of 0.3 mm. Both the rotor and the stator have been coated using electroless plating with a variety of metals: Rh, Pd, Pt, Au, and Cu. The rotation was effected by the insertion of a fan motor, controlled by a variac, into the rotor.

Experimental setup and parameters. A schematic of the experimental setup is presented in Fig. 1. A Japan-Inter uHV-10 ac high-voltage generator operating at 8.1 kHz was used to produce the voltage across the gap. The voltage and current conditions of the plasma were monitored using a Tektronix 6015A high-voltage probe and a Yokogawa DL1520 digital oscilloscope, and the current was monitored by measuring the voltage drop across a 10-Ω resistor placed in series using a test probe. An ac voltage of 400–900 V rms (root-mean-square) was placed across the gap between the rotor (ground) and the stator to produce the plasma, and the fan was operated at 3600 rpm. The plasmas were run at atmospheric pressure using a 2.5% CO_2 in He prepared mixture with gas flow rates of 30–100 cc/min. The plasma volume was approximately 0.25 cm^3. The gas temperature in the reactor was about 50°C, determined by inserting a temperature probe into the reactor immediately after shutting off the plasma.

Product analysis. The products were analyzed using an MKS-UTI PPT quadrupole residual gas analyzer mass spectrometer (MS) with a Faraday cup detector and a variable high-pressure sampling manifold. Conversion of CO_2 was obtained by monitoring the change in signal of the m/e 44 peak, which is proportional to the partial pressure of CO_2, as a function of the plasma conditions. The CO and O_2 products were quantified by monitoring the $m/e = 28$ and $m/e = 32$ signals, respectively.

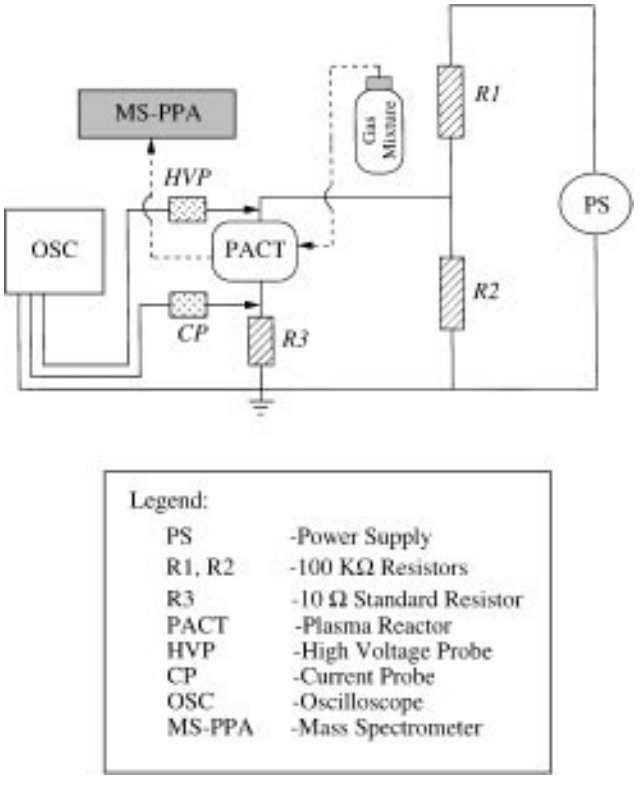

FIG. 1. Schematic of the experimental setup for generation of the plasma and monitoring of the voltage and current characteristics.

Emission (luminescence) spectroscopy. A 270-M Spex instrument with a CCD detector was used to obtain luminescence spectra of the plasmas. The light was collected with a fiber optic cable and directed into the monochromator. Studies were performed in the wavelength range 200–900 nm and the emission lines from helium are accurate to ±0.1 nm.

RESULTS

Voltage and current characterization of the plasma. The voltage characteristics of the reaction setup as a function of time are presented in Fig. 2 for both the open circuit (input voltage) and the closed circuit (plasma) conditions. Initiation of a plasma for a 2.5% CO_2 in He mixture occurs when the input voltage across the gap is increased above approximately 1 kV. When the plasma is initiated, the shape of the voltage curve closely follows that of the input voltage up to a particular voltage and then flattens out through the peak in the input voltage. The characteristic voltage

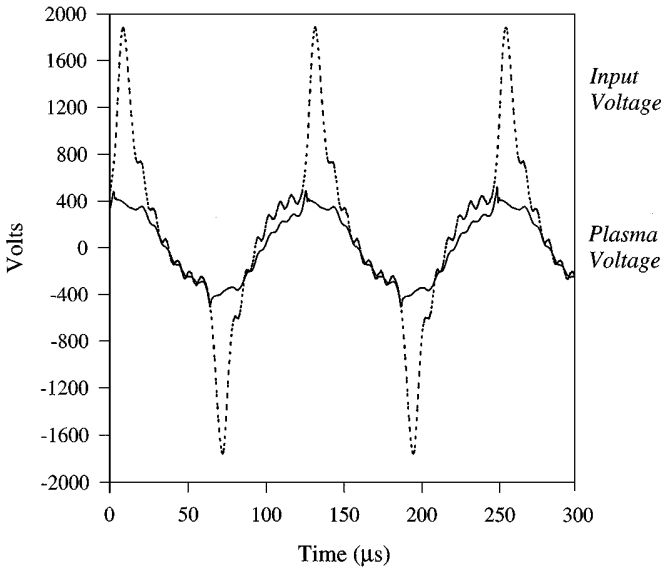

FIG. 2. Voltage vs time waveform for the open circuit input voltage and closed circuit plasma conditions for a 2.5% CO_2 in He mixture in a Cu reactor.

and current variables of the plasma are illustrated in Fig. 3. The breakdown voltage, V_s, corresponds to the maximum voltage achieved in the plasma. The glow voltage, V_g, is the voltage at which the signal flattens out (the normal glow region) and the glow period, t_g, is the duration of time for which V_g is maintained.

The flattening out of the signal is not absolute; the shape of the open circuit voltage curve is weakly superimposed in this region (Fig. 2). It is during this normal glow period of the ac cycle that the plasma is produced, resulting in a peak in the current waveform, also of width t_g. The small phase shift between the voltage and current waveforms is due to the capacitance of the system. Thus, the value of t_g represents the amount of time per 1/2 ac cycle that a plasma is present in the reactor. The peak current, i_p, corresponds to the maximum in the current. The power consumed by the reactor was determined by integrating the product of the voltage and current waveforms.

The voltage and current variables for the five reactors studied are presented in Table 1. The breakdown voltage and glow voltage are intrinsic functions of the reactor for the 2.5% CO_2 in He mixture used; they show some variation with respect to the identity of the metal catalyst coated onto the reactor but are independent of the input voltage applied. In contrast, the glow period, peak current, rms current and voltage, and the power consumed by the reactors are all linear functions of the input voltage and all increase with increasing input voltage.

Conversion, reaction rate, and efficiency of CO_2 decomposition. The decomposition of CO_2 in the different reactors was studied as a function of input voltage and flow rate of the 2.5% CO_2 in He gas. The changes in CO_2, CO,

TABLE 1

List of Plasma Variables as a Function of Input Voltage (V_{in} rms) and the Identity of the Metal Coating the Reactors

Metal	V_s (V)	V_g (V)	t_g (μs)	i_p (mA)	V_{rms} (V)	i_{rms} (mA)	Power (W)
			V_{in} rms = 411 V				
Au	480	360	13.6	26	236	5.7	0.766
Pd	600	390	11.7	14	261	5.9	0.744
Cu	500	380	13.2	20	244	4.3	0.710
Pt	600	420	11.5	14	249	5.3	0.606
Rh	570	370	14.0	24	252	6.0	0.714
			V_{in} rms = 711 V				
Au	480	360	18.6	36	275	11.5	1.85
Pd	600	390	16.1	35	290	13.0	1.89
Cu	500	380	17.4	34	285	10.0	1.66
Pt	600	420	16.2	35	278	11.5	1.79
Rh	520	360	17.0	35	272	12.0	1.95
			V_{in} rms = 906 V				
Au	480	360	21.0	42	303	14.0	2.57
Pd	590	390	19.8	43	305	16.3	2.64
Cu	500	380	20.4	40	305	13.4	2.37
Pt	600	420	19.3	42	295	14.0	2.58
Rh	520	360	20.6	42	300	14.8	2.85

Note. V_s, breakdown voltage; V_g, glow voltage; t_g, glow voltage period; i_p, peak current; V_{rms}, rms plasma voltage; i_{rms}, rms plasma current.

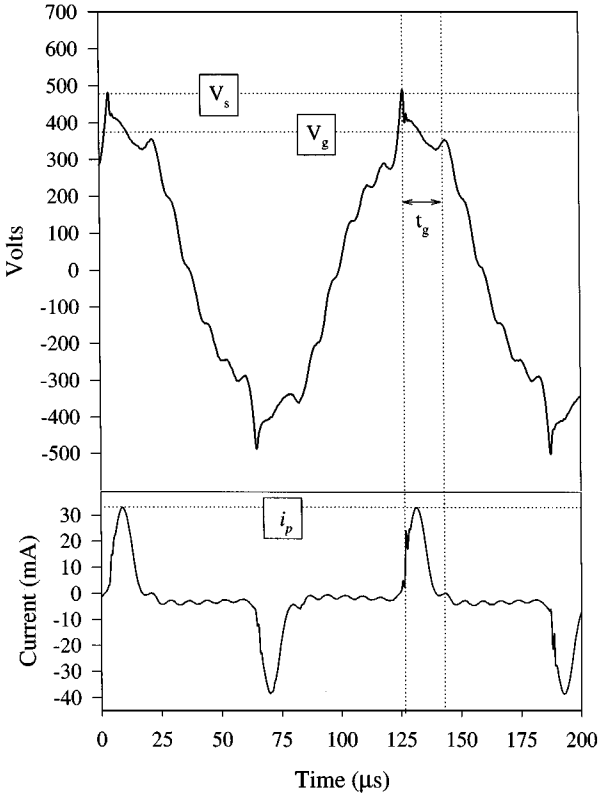

FIG. 3. Voltage and current vs time waveform for a 2.5% CO_2 in He mixture in a Cu reactor with plasma parameters illustrated. V_s, breakdown voltage; V_g, glow voltage; t_g, glow voltage period; i_p, peak current.

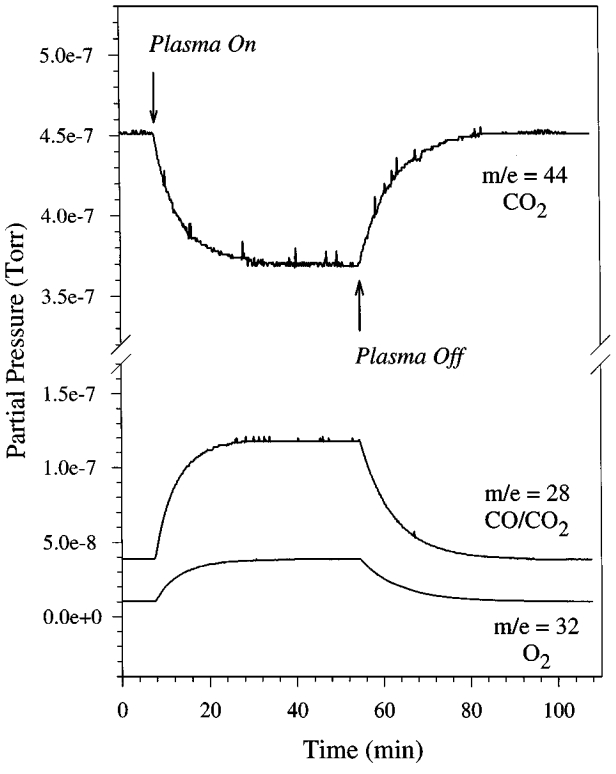

FIG. 4. Partial pressure of CO_2, CO, and O_2 as a function of time obtained from a mass spectrometer with a residual gas analyzer for an on/off plasma cycle. These data, obtained using a Cu reactor, are typical of all the reactors.

and O_2 concentrations in the exit stream were monitored with a mass spectrometer with a partial pressure analyzer (MS-PPA). The MS-PPA data for a reaction in the copper plated reactor, typical of all the reaction runs, are presented in Fig. 4. Initiation of the plasma results in a decrease in the $m/e = 44$ signal (CO_2) and a concomitant increase in the $m/e = 28$ (CO) and $m/e = 32$ (O_2) signals. There is a significant lag time, dependent on the flow rate, before a steady state value for conversion is obtained. The lag time decreases as the flow rate increases. When the plasma is shut off, the partial pressures of all the species return to their initial values. A scan of the mass range 1–100 revealed no other products, and no carbonaceous deposits were observed on the reactor after the reaction, even after running for 30 h. A carbon mass balance calculation for this reaction suggests selectivity to CO is in the range 80–95%.

The percentage conversion of CO_2 in the 2.5% CO_2 in He mixture as a function of the input voltage and the metal catalyst is presented in Fig. 5 and Table 2. The order of reactivity as a function of metal catalyst is Rh > Pt ≈ Cu > Pd > Au and is most obvious at high voltages where the largest differences in conversion and efficiency are observed. For an input voltage of 906 V rms, corresponding to 2.57–2.85 W, conversions of 30.5 and 15.2% were obtained for Rh and Au, respectively, at a flow rate of 30 cc/min. At 411 V rms

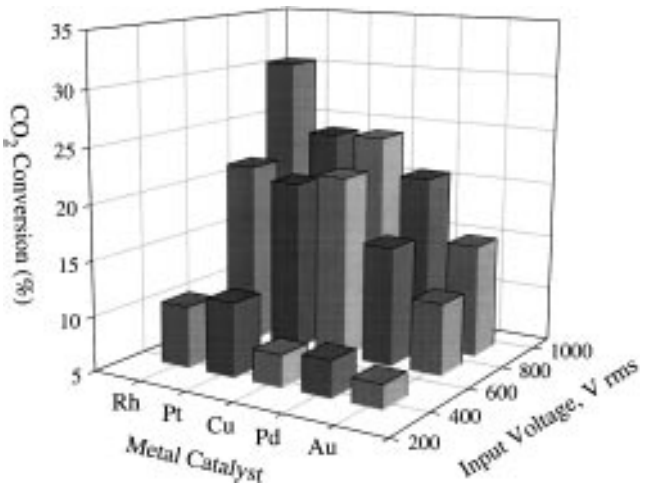

FIG. 5. Percentage conversion of CO_2 for a 2.5% CO_2 in He mixture as a function of input voltage and metal catalyst. The flow rate is 30 cc/min.

(0.714–0.766 W) the respective conversions are 10.6 and 7.2%.

The percentage conversion of CO_2 as a function of the flow rate for the catalytic reactors is plotted in Fig. 6 and the data are presented in Table 2. In all cases, an increase in flow rate corresponds to a decrease in the percentage conversion. The curves for all metals, with the exception of Pt, which is the only metal to show a linear dependence, resemble each other and do not cross.

The reactors were also evaluated with respect to the steady state reaction rate (mol/h) and the energy efficiency in percentages, defined as $100 \times E_c/E_p$, where E_c is the calculated free energy for the decomposition of CO_2 to CO and O_2 (257 kJ/mol) and E_p is the energy of the plasma (kJ) per mole of CO_2 consumed. The reaction rate data as a function of input voltage and flow rate are presented in

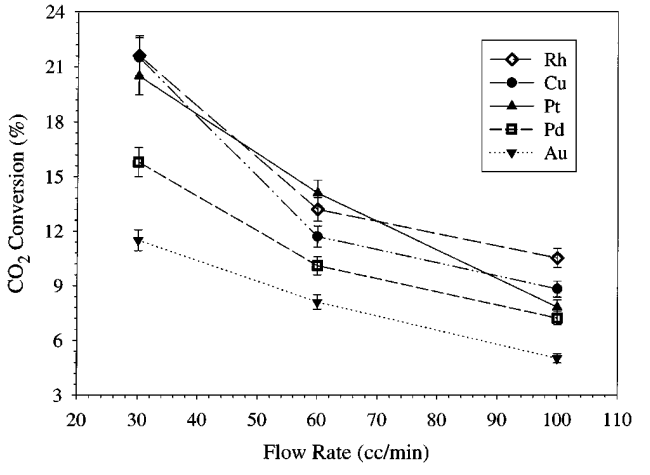

FIG. 6. Percentage conversion of CO_2 for a 2.5% CO_2 in He mixture as a function of flow rate of the reactant gas for various metal catalysts. The input voltage is 711 V, rms.

TABLE 2

Percentage Conversion of CO_2, Reaction Rate, and Percentage Efficiency[a] of CO_2 Dissociation as a Function of Metal Catalyst, Input Voltage, and Flow Rate for a 2.5% CO_2 in He Mixture

		Flow rate								
		30 cc/min			60 cc/min			100 cc/min		
Metal	V_{in} rms (V)	Conv. (%)	Rate $\times 10^4$ (mol/h)	Eff. (%)	Conv. (%)	Rate $\times 10^4$ (mol/h)	Eff. (%)	Conv. (%)	Rate $\times 10^4$ (mol/h)	Eff. (%)
Au	411	7.2	1.32	1.24	4.5	1.66	1.55	2.8	1.75	1.61
	711	11.5	2.14	0.82	8.1	3.02	1.16	5.0	3.09	1.18
	906	15.2	2.82	0.78	9.4	3.48	0.96	5.0	3.09	0.86
Pd	411	8.1	1.50	1.43	6.1	2.39	2.16	4.1	2.54	2.41
	711	15.8	2.91	1.10	10.1	3.93	1.41	7.2	4.48	1.67
	906	20.9	3.86	1.04	13.6	5.29	1.35	9.9	6.11	1.65
Cu	411	7.9	1.45	1.47	5.3	1.94	1.96	4.6	2.83	2.84
	711	21.5	3.81	1.65	11.7	4.32	1.86	8.8	5.38	2.31
	906	24.2	4.46	1.35	16.4	6.01	1.65	12.4	7.61	2.30
Pt	411	11.7	2.16	2.53	7.8	2.89	3.40	3.8	2.36	2.75
	711	20.5	3.77	1.51	14.1	5.20	2.08	7.8	4.82	1.90
	906	24.1	4.45	1.24	16.7	6.18	1.71	11.1	6.86	1.88
Rh	411	10.6	1.95	1.96	6.9	2.54	2.55	5.8	3.75	3.55
	711	21.6	4.00	1.45	13.2	4.89	1.79	10.5	6.93	2.35
	906	30.5	5.66	1.41	16.6	6.16	1.53	12.4	8.07	1.90

Note. The standard deviations for the conversion, rate, and efficiency are $\leq 5\%$ of the value.

[a] Percentage efficiency calculated as $100 * E_c/E_p$. E_c is the calculated free energy for $CO_2 \rightarrow CO + O$ (257 kJ/mol); E_p is the plasma energy (kJ) per mole of CO_2 consumed.

Table 2. At constant flow rate, the steady state reaction rate follows the conversion trend and increases with increasing input voltage. However, when the flow rate is increased, the reaction rate also increases, in contrast to the trend for conversion. The percentage efficiency as a function of input voltage is also presented in Table 2. With the exception of the Cu-coated reactor, which shows the best efficiency at an intermediate voltage of 711 V rms, all of the reactors show an increase in efficiency with decreasing input voltage and the largest change comes between 711 and 411 V rms. This trend is opposite to that obtained for percentage conversion. A plot of the percentage efficiency as a function of flow rate for the various reactors is presented in Fig. 7 and the data are presented in Table 2. In this case, the Pt-coated reactor is the exception to the rule, with the largest efficiency corresponding to a flow rate of 60 cc/min. All of the other reactors have maximum efficiencies at 100 cc/min and the efficiency decreases with decreasing flow rate, again in contrast to the trend observed for percentage conversion.

To further probe the catalytic effect of the metals employed in this study, reactors composed of rotors and stators with different catalytic coatings were assembled. Au and Rh were chosen, as these metals demonstrate the worst and best CO_2 conversion, respectively, in our system. Two reactors were prepared, one composed of stator/rotor Au/Rh and one of Rh/Au. Both reactors gave nearly identical conversions: 17.4% for Au/Rh and 16.8% for Rh/Au for a flow rate of 30 cc/min and an input voltage of 906 V rms. These conversions are only marginally better than those obtained with the pure gold reactor (15.2%) and considerably poorer than those obtained with a pure Rh reactor (30.5%).

In addition to He, both Ar and N_2 were investigated as diluent gases. The results are presented in Table 3. The conversion and reaction rate order for CO_2 as a function of diluent gas is $He > Ar > N_2$. Additionally, the power

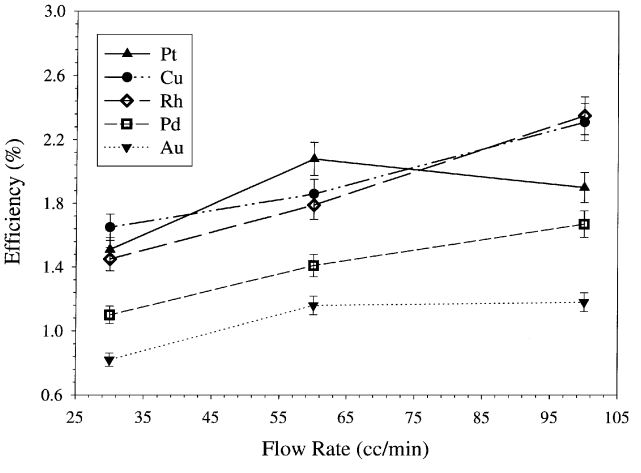

FIG. 7. Percentage efficiency as a function of flow rate of the 2.5% CO_2 in He reactant mixture for various metal catalysts. The input voltage is 711 V, rms.

TABLE 3

Plasma Power, Percentage Conversion of CO_2, Reaction Rate, and Percentage Efficiency[a] Data for CO_2 Decomposition as a Function of Diluent Gas

		Flow rate								
		30 cc/min			60 cc/min			100 cc/min		
Diluent gas	Plasma power (W)	Conv. (%)	Rate $\times 10^4$ (mol/h)	Eff. (%)	Conv. (%)	Rate $\times 10^4$ (mol/h)	Eff. (%)	Conv. (%)	Rate $\times 10^4$ (mol/h)	Eff. (%)
He	2.78	30.5	5.61	1.44	16.6	6.11	1.57	12.4	7.60	1.95
Ar	3.64	19.6	3.61	0.64	11.5	4.23	0.83	7.01	4.30	0.96
N_2	5.25	13.5	2.48	0.35	9.16	3.37	0.44	6.17	3.78	0.51

Note. The 2.5% CO_2 in He, Rh reactor, $V_{in} = 906$ V rms. The standard deviations for conversion, rate, and efficiency are $\leq 5\%$ of the values.

[a] Percentage efficiency calculated as $100 * E_c/E_p$. E_c is the calculated free energy for $CO_2 \rightarrow CO + O$ (257 kJ/mol); E_p is the plasma energy (kJ) per mole of CO_2 consumed.

consumption is lowest and the percentage efficiency highest when He is the diluent gas.

Spectroscopic studies. Emission spectra of pure He plasmas and plasmas of CO_2 mixtures in He were obtained and the results are presented in Fig. 8. As small amounts of CO_2 are added to the feed, the relative intensities of the He lines are observed to change considerably. Additionally, small broad peaks with vibrational structure due to emission from CO^+ (not shown) and CO_2^+ (see inset) grow in. The same relative intensity of He lines was observed regardless of the metal when 2.5% CO_2 was present; however, the spectra of pure He were observed to vary considerably as a function of the metal catalyst. The Boltzmann plot method (24) was used to calculate the excitation temperature, T_{ex}, for a pure He plasma as a function of catalyst metal. The relationship between T_{ex} for a pure He plasma (which should be proportional to the electron temperature) and percentage conversion of CO_2 in a 2.5% CO_2 in He mixture is presented in Fig. 9. The data indicate that T_{ex} and conversion are inversely correlated, so that the best conversion is obtained for the lowest excitation temperature. The Rh- and Pt-coated reactors have the lowest values of T_{ex}, 1880 and 1840 K, respectively, corresponding to conversion values of 30.5 and 24.1%. The highest excitation temperature is obtained with the gold-coated reactor (2460 K), which corresponds to 15.2% conversion.

DISCUSSION

Reaction and mechanism. The use of efficiency values normalizes the effects of flow rate, input voltage, and power on the conversion. High selectivity toward CO (>80%) justifies the calculation. The trends for efficiency as a function of power (Table 2) and flow rate (Fig. 7) are opposite those for conversion; i.e., efficiency increases with decreasing input voltage (or power) and increasing flow rate. This phenomenon originates in the fact that the correspondence between conversion and input voltage (power), or conversion and flow rate, is less than 1 : 1. Thus, a doubling of the input voltage (or halving of the flow rate) produces less than a doubling of conversion. Additionally, the dependence of

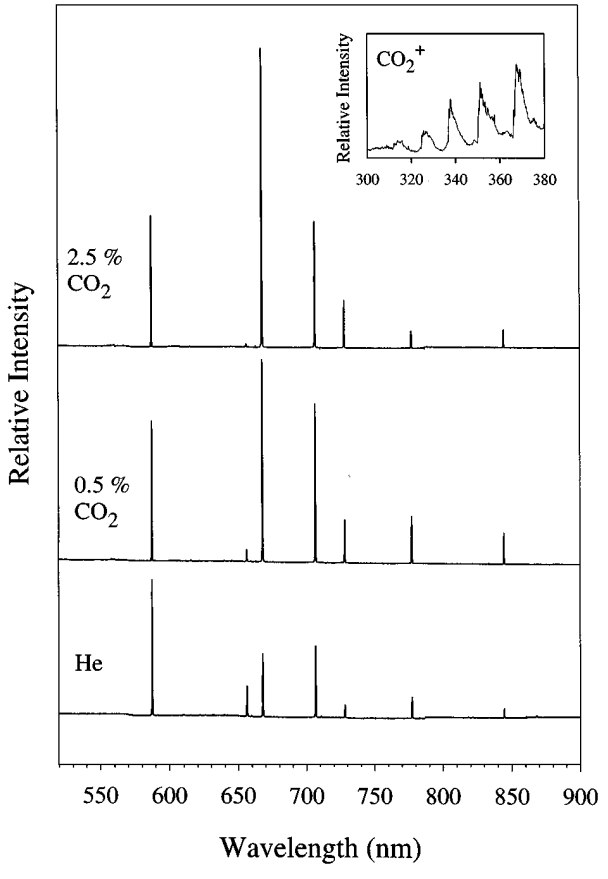

FIG. 8. Optical emission spectra for pure He, 0.5% CO_2 in He, and 2.5% CO_2 in He reactant gases obtained with a gold-coated reactor ($V_{in} = 1.07$ kV, rms; flow rate = 30 cc/min). The $A^2\Pi_u \rightarrow X^2\Pi_g$ excited state CO^{2+} bands (see inset) exhibit fine structure which has been attributed to bending modes generated by collisions with He^+.

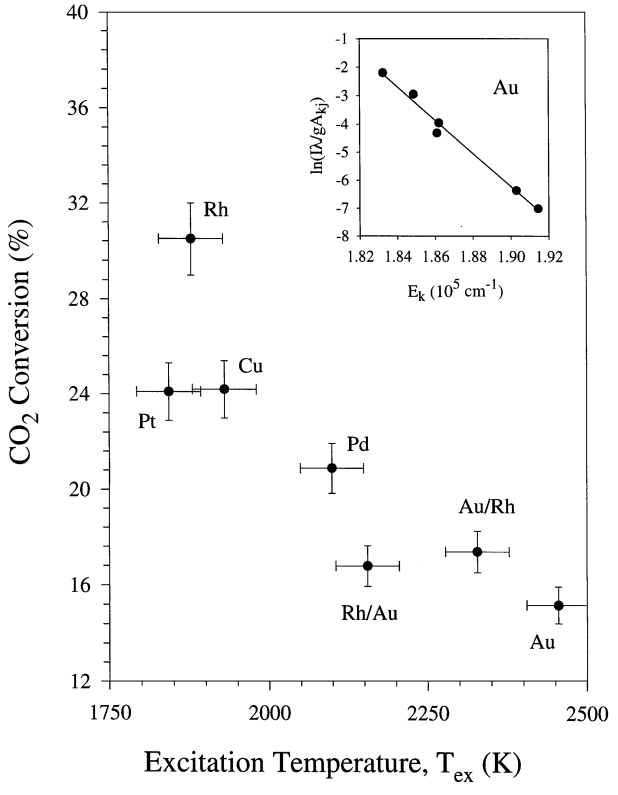

FIG. 9. Conversion of CO_2 as a function of excitation temperature, T_{ex}, for the various metal reactors studied. T_{ex} is obtained from a plot of $\ln(I\lambda/gA_{kj})$ vs E_k (see inset) where I is the intensity of the He line, g is the statistical weight of the level, A_{kj} is the transition probability, and E_k is the excitation energy of the upper level. Note that for ionizing plasmas, not in local thermodynamic equilibrium, $T_{ex} > T_e$ (electron temperature). See Ref. (24) for further discussion.

conversion on input voltage and flow rate is generally nonlinear (a shallow curve); thus increased input voltage or decreased flow rate yields diminishing returns.

The fact that the correspondence between the energy supplied to the plasma and the conversion is less than one has to do with how the energy is distributed within the plasma. Specifically, pathways that produce vibrationally excited CO_2 favor subsequent dissociation. The decrease in efficiency as the input voltage is increased suggests that the energy distribution is changing in the plasma as a function of input voltage. Perhaps a greater fraction of the input energy results in heat production, which is detrimental for CO_2 dissociation. The flow rate dependence of the efficiency may be a function of the reversibility of the CO_2 dissociation reaction. The rate of the reverse reaction will depend on the concentrations of CO_2, CO, and O_2 in the plasma zone and on the space velocity. At low flow rates, it would appear that the reverse reaction rate has increased relative to the forward reaction rate, resulting in lower efficiencies. The best efficiency obtained is 3.55%, corresponding to a reduction of 23.1 g/k Wh. This value is about a quarter of that obtained by Chang and co-workers using an ac ferroelectric packed bed reactor, but our selectivity to CO appears to be considerably higher, as Chang and co-workers observed carbonaceous deposits on the surface of the dielectric particles after the reaction (14).

The reaction rate is normalized only with respect to flow rate; thus, it correlates directly with the conversion as a function of input voltage. With respect to flow rate, at constant input voltage, the increase in flow rate more than compensates for the decrease in conversion, resulting in an increase in the reaction rate. Thus, the highest rate of reaction is 8.07×10^{-4} mol/h, obtained for the Rh reactor at 906 V_{in} rms and 100 cc/min.

Decomposition of pure CO_2 in a plasma generally follows one of two reaction pathways involving electron impact (16),

$$CO_2 + e^- \rightarrow CO + O + e^- \quad [1]$$

$$CO_2 + e^- \rightarrow C + O_2 + e^-, \quad [2]$$

with the branching of [1] and [2] depending on the vibrational excited state of CO_2. However, in the presence of diluent gases such as He, Ar, and N_2, a third pathway involving charge and energy transfer via ionic collisions is possible, illustrated for the case of He in the equations (16, 25)

$$He + e^- \rightarrow He^+ + 2e^- \quad [3]$$

$$He^+ + 2He \rightarrow He_2^+ + He \quad [4]$$

$$He^+ (\text{or } He_2^+) + CO_2 \rightarrow CO_2^+ + He \text{ (or } 2He) \quad [5]$$

$$CO_2^+ + e^- \rightarrow CO + O. \quad [6]$$

In this third pathway, coke is not formed as a product. From the spectroscopic data it is clear that He plays an important role in the reaction. As CO_2 is introduced to the reaction, the relative population of excited states of He changes, evidenced by a change in relative intensity of the He emission lines. This is consistent with a decomposition pathway involving charge and energy transfer from He species such as He^+ or He_2^+ to CO_2. The presence of vibrationally excited CO_2^+ in the $A^2\Pi_u \rightarrow X^2\Pi_g$ state is also consistent with this hypothesis, as this vibrational excitation is purported to arise uniquely from collision of He^+ with CO_2 (26). Such vibrational excitation, according to Polyani's rules, is mandatory to drive the endothermic dissociation of CO_2 to CO (13, 27).

If a charge and energy transfer mechanism is in effect, the identity of the diluent gas would be expected to have a profound effect on the reaction, and we have found this to be so (see Table 3). The Rh-coated reactor operating at 906 V rms input and a flow rate of 30 cc/min yields conversions of 30.5, 19.6, and 13.5% for He, Ar, and N_2, respectively. This order of reactivity is consistent with the rate constants for bimolecular energy transfer from the diluent gas to CO_2: 16×10^{-10} cm^3/s (He_2^+) (25), 11×10^{-10} cm^3/s (Ar_2^+) (16),

and 7.7×10^{-10} cm^3/s (N_2^+) (16). Thus, as other authors have observed, diluent gases are not passive components of the plasma, but can be used to control the reactivity (11, 16). He as a diluent gas is found to yield the best conversions and the highest reaction efficiencies in our system.

Metal effect. It is clear from the data presented here that the metal catalyst has a pronounced effect on the breakdown of CO_2 in the plasma. Similar studies in metal- and glass-coated tubular plasma reactors indicate increased reactivity for plasma reactors with metal coatings relative to glass (28). While the design of the reactor described here is not suitable for glass electrodes, it is possible to compare the effects of a number of different metal catalysts. A clear trend in reactivity is observed in both the conversion and efficiency data as a function of catalyst metal: Rh > Pt ≈ Cu > Pd > Au. Spectroscopically, this order is well reflected in the excitation temperatures obtained for pure He plasmas in the five coated reactors. Lower excitation temperatures translate to higher CO_2 conversions, which may indicate that the He species responsible for charge and energy transfer are of relatively low energy. For mixed metal Au/Rh systems, the Au seems to have the effect of dampening the reactivity and this is also seen in the excitation temperatures of these systems. Like the conversion values, the excitation temperatures fall between those for the Pd- and Au-plated reactors.

Catalytic effects of metals, oxides, and even polymers have been reported in the literature and the effects have been attributed to both plasma species/surface interaction and the ability of the coating to modify the electrical characteristics of the plasma (22, 23, 29, 30). Specifically, electron work function and surface effects such as absorption–desorption have been cited as important plasma/surface effects governing the reactivity, and the macroscopic electrical parameters may control the voltage/current characteristics of the plasma, permitting a favorable pathway to products. We have found no correlation between the conversion and the work function of the metal, nor have we been able to attribute the variation in reactivity to any specific property of the metal electrode. It is likely that the differences are due to the contributions of a number of different intrinsic parameters, such as specific heat, sticking coefficient, and ionization potential. Furthermore, the surfaces of the metals, with the exception of Au, are oxidized and thus surface properties may be difficult to predict. A combination of such effects may explain some of the unusual results observed for the Pt- and Cu-coated reactors. Sputtering may also occur, which may explain the similarity of the Au/Rh (Rh/Au) system to the pure Au system. Conductive particles in the feed are known to adversely affect the dielectric strength of the gas, resulting in lower reactivity (31). However, we have detected no signs of sputtering, either spectroscopically or from XPS studies of a copper plate placed at the back of the Au/Rh-coated reactor which were unable to verify the presence of either Au or Rh sputtered atoms or clusters.

CONCLUSIONS

Conversions of CO_2 to produce CO and O_2 up to 30.5% with >80% selectivity, reaction rates of up to 8.07×10^{-4} mol/h, and energy efficiencies as high as 3.55% have been realized in fan-type plasma reactors using a test gas mixture of 2.5% CO_2 in He. The conversion of CO_2 increases with increasing input voltage (power) and decreasing flow rate and the efficiency of the reactors show opposite trends. The reaction rate increases with both increasing input voltage and flow rate. The most likely mechanism of dissociation involves charge and energy transfer from excited state He to CO_2 to form CO_2^+ in a vibrationally excited state. Subsequent electron impact causes dissociation to form CO + O, and He is found to yield the highest conversions and efficiencies, relative to Ar and N_2. A metal effect is clear from analysis of the conversion, reaction rate, efficiency, and spectroscopic data, though we have been unable to correlate such an effect with any intrinsic metal properties. A relative reactivity order of Rh > Pt ≈ Cu > Pd > Au/Rh ≈ Rh/Au ≈ Au has been obtained for the metal-plated reactors. Further studies are under way, including highly correlated quantum–chemical *ab initio* calculations, to gain further insight into the role of the metal catalyst in CO_2 plasma decomposition. Additionally, we are investigating the effects of other plasma parameters on the dissociation of CO_2, such as frequency and CO_2 concentration, with the goal of increasing the conversion, reaction rate, and efficiency of the reaction.

ACKNOWLEDGMENTS

The authors thank Ms. Tomoko Shimojo for reproducing some of the data presented here, Dr. Venkat V. Krishnan for assistance in setting up the MS system, Mr. Guanguang Xia for help designing the electrical circuit, and Mr. Jeff Rozak for assistance with the power measurements. Additionally, the authors acknowledge helpful discussions with Professor G. Roussy of Université Postal Henri Poincaré, Professor J. K. S. Wan of Queen's University, R. Meyer of ASTEX, Inc., and M. C. Quintero and A. Sola of the University of Córdoba. We thank all the researchers involved in the *p*lasma *a*nd *c*atalytic *i*ntegrated *t*echnologies (PACT) Japanese–American collaboration and Honda Research and Development Corp., Fujitsu Ltd., and Hokushin Co. for support of this research.

REFERENCES

1. Edwards, J. H., *Catal. Today* **23**, 59 (1995).
2. Azar, C., and Rodhe, H., *Science* **276**, 1818 (1997).
3. Sellers, P. J., Bounoua, L., Collatz, G. J., Randall, D. A., Dazlich, D. A., Los, S. O., Berry, J. A., Fung, I., Tucker, C. J., Field, C. B., and Jensen, T. G., *Science* **271**, 1402 (1996).
4. Knutson, T. R., Tuleya, R. E., and Kurihara, Y., *Science* **279**, 1018 (1998).
5. Inui, T., *Catal. Today* **29**, 329 (1996).
6. Papp, H., Schuler, P., and Zhuang, Q., *Topics Catal.* **3**, 299 (1996).

7. Chang, J.-S., Park, S.-E., and Chon, H., *Appl. Catal. A* **145**, 111 (1996).
8. Mark, M. F., and Maier, W. F., *J. Catal.* **164**, 122 (1996).
9. Fisher, I. A., and Bell, A. T., *J. Catal.* **162**, 54 (1996).
10. Cenian, A., Chernukho, A., Borodin, V., and Sliwinski, G., *Contrib. Plasma Phys.* **34**, 25 (1994).
11. Buser, R. G., and Sullivan, J. J., *J. Appl. Phys.* **41**, 472 (1979).
12. Andreev, Y. P., Voronkov, Y. M., and Semiokhin, I. A., *Russ. J. Phys. Chem.* **49**, 394 (1975).
13. Fridman, A. A., and Rusanov, V. D., *Pure Appl. Chem.* **66**, 1267 (1994).
14. Jogan, K., Mizuno, A., Yamamoto, T., and Chang, J.-S., *IEEE Trans. Ind. App.* **29**, 876 (1993).
15. Barton, M. J., and Von Engel, A., *Phys. Lett. A* **32**, 173 (1970).
16. Maezono, I., and Chang, J.-S., *IEEE Trans. Ind. App.* **26**, 651 (1990).
17. Huang, J., and Suib, S. L., *J. Phys. Chem.* **97**, 9403 (1993).
18. Marun, C., Suib, S. L., Dery, M., Harrison, J. B., and Kablaoui, M., *J. Phys. Chem.* **100**, 17,866 (1996).
19. Giraldo, O. H., Willis, W. S., Marquez, M., Suib, S. L., Hayashi, Y., and Matsumoto, H., *Chem. Mater.* **10**, 366 (1998).
20. Hayashi, Y., U.S. Patent 08/139,907, Fujitsu Ltd., July (1995).
21. Hayashi, Y., Ohta, H., and Yanobe, T., U.S. Patent 08/278,069, Hokushin Co., Fujitsu Ltd., August (1995).
22. Suhr, J., and Weddigen, G., *Combust. Sci. Tech.* **72**, 101 (1990).
23. Tanaka, S., Uyama, H., and Matsumoto, O., *Plasma Chem. Plasma Proc.* **14**, 491 (1994).
24. Quintero, M. C., Rodero, A., Garcia, M. C., and Sola, A., *Appl. Spectrosc.* **51**, 778 (1997).
25. Lee, F. W., Collins, C. B., and Waller, R. A., *J. Chem. Phys.* **65**, 1605 (1976).
26. Sim, W., and Haugh, M., *J. Chem. Phys.* **65**, 1616 (1976).
27. Capezzuto, P., Cramarossa, F., d'Agostino, R., and Molinari, E., *J. Phys. Chem.* **80**, 882 (1976).
28. Luo, J., Suib, S. L., Hayashi, Y., and Matsumoto, H., *J. Catal.*, in press.
29. Gicquel, A., Cavadias, S., and Amouroux, J., *J. Phys. D Appl. Phys.* **19**, 2013 (1986).
30. Schmidt-Szalowski, K., and Borucka, A., *Plasma Chem. Plasma Proc.* **9**, 235 (1989).
31. Pace, M. O., Adcock, J. L., Frees, L. C., and Christophorou, L. G., *in* "Gaseous Dielectrics. III. Proceedings of the 3rd International Symposium on Gaseous Dielectrics" (L. G. Christophorou, Ed.), p. 307. Pergamon, New York, 1982.